Progress In Electromagnetics Research, Vol. 112, 183–197, 2011

TRANSIENT RESPONSE CHARACTERIZATION OF THE HIGH-SPEED INTERCONNECTION RLCG-MODEL FOR THE SIGNAL INTEGRITY ANALYSIS

T. Eudes, B. Ravelo, and A. Louis

IRSEEM, EA 4353, Engineering School ESIGELEC
Technopole de Madrillet
Avenue Galilée, BP 10024
76801 Saint-Etienne-du-Rouvray Cedex, France

Abstract—This paper is devoted on the characterization method of RF/digital PCB interconnections for the prediction of the high-speed signal transient responses. The introduced method is based on the use of the interconnection line RLCG-model. Theoretical formulae enabling the extraction of the electrical per-unit length parameters R, L, C and G in function of the interconnection line physical characteristics (width, length, metal conductivity, dielectric permittivity ...) are established. Then, by considering the second order approximation of the interconnection RLCG-model transfer matrix, the calculation process of the transient responses from the interconnection system transfer function is originally established. To demonstrate the relevance of the proposed model, microwave-digital interconnection structure comprised of millimetre microstrip line driven and loaded by logic gates which are respectively modelled by their input and output impedances was considered. Then, comparisons between the SPICE-computation results and those obtained from the proposed analytical model implemented in Matlab were made. As results, by considering a periodical square microwave-digital excitation signal with 2 Gbits/s rate, transient responses which are very well-correlated to the SPICE-results and showing the degradation of the tested signal fidelity are observed. The numerical computations confirm that the proposed modelling method enables also to evaluate accurately the transient signal parameters as the rise-/fall-times and the 50% propagation delay in very less computation time. For this reason, this analytical-numerical modelling method is potentially interesting for the analysis of the signal integrity which propagates

Received 18 November 2010, Accepted 9 December 2010, Scheduled 12 January 2011
Corresponding author: Blaise Ravelo (blaise.ravelo@esigelec.fr).

in the high-speed complex interconnection systems as the clock tree distribution networks. In the continuation of this work, we would like to apply the proposed modelling process for the enhancement of signal quality degraded by the RF/digital circuit board interconnection where the signal delays and losses became considerably critical.

1. INTRODUCTION

The last century was particularly remarkable with the spectacular progress of the microelectronic semiconductor industries which was till now, unique in the mankind history. These constant technological progresses are nowadays a source of innovative product developments in numerous civil sectors as the mobile phones, multimedia systems, medical equipments and even vehicles. As an undeniable quantification of this industrial development, according to Moore's law prediction, at each generation the size of electronic printed circuit board (PCB) is reduced of 30% and every two or three years, the number of the transistors integrated in the microelectronic chips must be increased of four times [1]. Despite this fascinating scenario of technological development, the structures of the current interconnection circuitry between the logic gates, electronic chips and digital devices, and even the buses linking the different electronic boards as seen in Fig. 1 become more and more complicated [2–7].

Figure 1. High speed digital PCB.

Furthermore, due to the incessant increase of the operating frequencies and the integration density, the contributions of the interconnection electric parameters as the resistance, capacitance and inductance effects [8–15] cannot presently be neglected by the electronic equipment manufacturers. Indeed, the signal integrity which represents the numerical-/digital-data is not preserved especially for the high-rate communication. This signal degradation effect needs to be taken into account by the electronic designers during the manufacture processes of the high-speed electronic devices. For this

reason, different characterization techniques of the interconnection transmission line (TL) based on the S-parameter extractions were introduced since two decades ago [16–21]. In this optic, performance optimization methods dedicated to the clock tree distribution networks were proposed [22–24] in order to minimize the undesired influences of interconnection systems notably for the VLSI circuits. In addition, a compensation technique based on the insertion of repeaters between the piece of TLs was also proposed [11, 25] in order to reduce the TL interconnection negative effects. As improvement of this interconnection compensation technique, an alternative solution based on the use of negative group delay (NGD) circuits is introduced in [26, 27].

Notwithstanding these various technical solutions, further simpler, faster and more accurate methods need to be developed to model the interconnection line effects especially for the complex circuitry especially, in transient domain. One underlines that most of existing characterization methods were developed only in frequency domain by using the S-parameter characterization deduced from the geometrical parameters (width, length, substrate height) of the TL and the electromagnetic properties (dielectric permittivity and metal resistivity) [16–20, 28]. Whereas the existing time-domain characterization methods are usually based on the use of the classical RC- or RLC-transfer function models [8–15, 29]. So, more complete modelling method is still necessary for the estimation of the transient response induced by the interconnection TLs particularly for the high-speed digital- and/or mixed-electronic systems.

This statement motivates us to suggest and to develop further modelling process allowing to forecast simply the influences of RF/digital interconnection circuitries on the signal quality via the analysis of the transient response behaviours. To make this paper more understandable, the theoretic analysis highlighting the determination of the microstrip TL high frequency parameters as the characteristic impedance and constant propagation from the geometrical (width, length, substrate height) and physical (dielectric permittivity and metal resistivity) characteristics is recalled in Section 2. Then, the calculation method enabling the extraction of the RLCG-model per unit length parameters is equally presented. Hence, mathematical analysis explaining the determination of the linear transfer function enabling to express the interconnection transient responses is offered in Section 3. Hence, discussions on validation results based on the comparison with standard electronic simulation tool SPICE results are the object of Section 4. Finally, the last Section is the conclusion of the paper.

2. EXTRACTION OF THE MICROSTRIP LINE RLCG-PARAMETERS

For starting let us consider the microstrip TL with geometrical length d, width w, metallisation thickness t as depicted in Fig. 2. One assumes that the dielectric substrate is characterized by its height h, relative permittivity ε_r and loss constant $\tan(\delta)$.

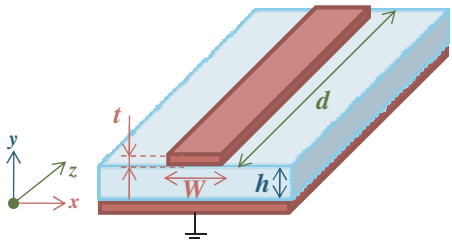

Figure 2. Geometrical representation of microstrip TL.

The corresponding characteristic impedance Z_c and the propagation constant $\gamma(f) = \alpha(f) + j \cdot \beta(f)$ can be deduced from these physical properties according to the formulations reported in [16, 17, 32] as expressed in (1) and (3).

$$Z_c = \frac{\eta_0}{2\pi\sqrt{\varepsilon_{eff}}} \ln\left[\frac{h \cdot a(w/h)}{w} + \sqrt{1 + \frac{4h^2}{w^2}}\right], \tag{1}$$

where

$$a(w/h) = 6 + (2\pi - 6) \cdot \exp\left[-\left(\frac{30.66h}{w}\right)^{0.7528}\right], \tag{2}$$

with η_0 is the air impedance and ε_{eff} is the effective permittivity of the medium. One points out that as reported in [32], by denoting c is the speed of light in the vacuum, the constant propagation:

$$\gamma(f) = \alpha_c(f) + \alpha_d(f) + j\frac{2\pi f}{c}\sqrt{\varepsilon_r(f)}, \tag{3}$$

includes the metallic conductor and the dielectric losses respectively given by:

$$\alpha_c(f) = 1.38 \cdot \left\{1 + \frac{h}{w_{eff}} \cdot \left[1 + \frac{1}{\pi} \cdot \ln\left(\frac{2h}{t}\right)\right]\right\} \cdot \frac{R_s(f)}{h \cdot Z_c(f)} \cdot \frac{32 - \left(\frac{w}{h}\right)^2}{32 + \left(\frac{w}{h}\right)^2}, \tag{4}$$

$$\alpha_d(f) = 27.3\frac{\varepsilon_r}{\varepsilon_r - 1} \cdot \frac{\varepsilon_{eff} - 1}{\sqrt{\varepsilon_{eff}}} \cdot \frac{\tan(\delta)}{\frac{2\pi f}{c}}, \tag{5}$$

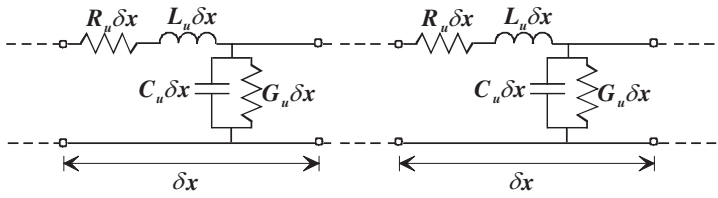

Figure 3. TL RLCG-model.

with

$$R_s(f) = \sqrt{\pi \cdot \mu_0 \cdot \rho \cdot f}, \tag{6}$$

$$w_{eff} = \begin{cases} w + \frac{1.25}{\pi}\left[1 + \ln\left(\frac{2h}{t}\right)\right], & if \quad \frac{w}{h} < \frac{1}{2\pi} \\ w + \frac{1.25}{\pi}\left[1 + \ln\left(\frac{4\pi w}{t}\right)\right], & if \quad \frac{w}{h} \geq \frac{1}{2\pi} \end{cases} . \tag{7}$$

For the calculations including the radiating loss, more explicit analytical expressions of the propagation constant real part or the per unit length loss constant $\alpha(f)$ are presented in [30–33]. Knowing Z_c and $\gamma(f)$, one can extract the equivalent TL RLCG-model with the per unit-length parameters R_u, L_u, C_u and G_u as described in Fig. 3. As established in [28], the TL global parameters $R = R_u \cdot d$, $L = L_u \cdot d$, $C = C_u \cdot d$, and $G = G_u \cdot d$ can be calculated with the following expressions:

$$R = \Re\left[\gamma(f) \cdot Z_c\right], \tag{8}$$

$$L = \frac{\Im\left[\gamma(f) \cdot Z_c\right]}{\omega}, \tag{9}$$

$$C = \frac{\Im\left[\frac{\gamma(f)}{Z_c}\right]}{\omega}, \tag{10}$$

$$G = \Re\left[\frac{\gamma(f)}{Z_c}\right], \tag{11}$$

where $\Re[z]$ and $\Im[z]$ are respectively the real and imaginary parts of the complex number z, and $\omega = 2\pi f$ is the operating angular frequency.

By denoting ρ the resistivity of the metallic conductor constituting the TL structure, it yields from the previous expressions that the global RLCG-parameter can be written as follows:

$$R = \frac{d\sqrt{\pi \cdot \mu_0 \cdot \rho \cdot f}}{w}, \tag{12}$$

$$L = \frac{d \cdot Z_c}{c}\sqrt{\varepsilon_{eff}}, \tag{13}$$

$$C = \frac{d\sqrt{\varepsilon_{eff}}}{c \cdot Z_c}, \tag{14}$$

$$G = d \cdot \tan(\delta) \cdot \omega \cdot C, \tag{15}$$

where μ_0 is the vacuum permeability. By using these parameter definitions, one proposes to establish the second order transfer function of the microstrip line before the determination of the TL transient responses.

3. POLYNOMIAL MODELLING OF THE MICROSTRIP INTERCONNECTION TL TRANSFER FUNCTION

As example of numerical-digital interconnection circuitry [11, 25–27], let us consider the microwave-digital system comprised of a TL driven and loaded by logic gates represented in Fig. 4. As can be seen here, the TL is characterized by its parameters (Z_c, γ) and its physical length d. One assumes that the driven gate output behaviour is consisted of a voltage source V_s with series impedance Z_s and the load gate as its input impedance denoted Z_L. According to the microwave theory, the transfer matrix of the interconnection line characterized by (Z_c, γ) with geometrical length d is expressed as:

$$[T_{TL}] = \begin{bmatrix} \cosh(\gamma \cdot d) & Z_c \sinh(\gamma \cdot d) \\ \frac{\sinh(\gamma \cdot d)}{Z_c} & \cosh(\gamma \cdot d) \end{bmatrix}. \tag{16}$$

By considering the RLCG-modelling behaviour depicted in Fig. 3, the overall interconnect system presented in Fig. 4 will be naturally transformed as shown in Fig. 5.

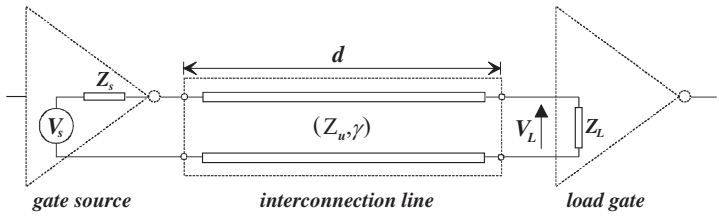

Figure 4. Interconnection TL driven and loaded by logic gates.

According to the signal processing theory, the frequency band of any digital signals is delimited by its theoretical bandwidth where belongs more than 85% of the baseband harmonic components [30]. Thus, it was established that for the square wave digital signal presenting rise-/fall-times t_r the frequency band is usually approximately equal to:

$$f_{\max} \approx \frac{0.35}{t_r}. \tag{17}$$

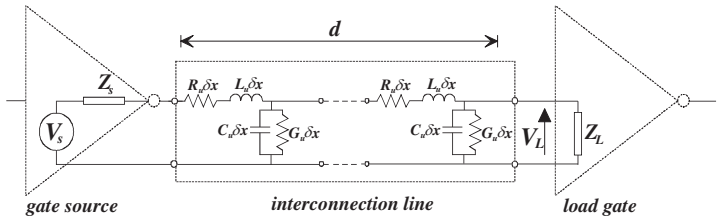

Figure 5. Interconnection RLCG-model driven by a voltage source V_s with inner impedance Z_s and loaded by Z_L.

It means that to study the analog-digital systems, one can consider its transfer function behaviour from DC to $f_{\max}$. More generally, one can take into account the transfer matrix of the TL as its baseband modelling behaviour by exploiting for example, the equivalent polynomial expression of the matrix $[T_{TL}]$. This approximation can be realized for example, by applying the second order MacLaurin expanding of each element of the transfer matrix. Therefore, one obtains the following expression:

$$[T_{TL}] \approx \begin{bmatrix} 1 + \frac{Z(s)\cdot Y(s)}{2} & Z(s) \\ Y(s) & 1 + \frac{Z(s)\cdot Y(s)}{2} \end{bmatrix}, \tag{18}$$

with $Z(s) = R + L \cdot s$ and $Y(s) = G + C \cdot s$. Therefore, according to the theory of electronic circuit and system, the overall transfer matrix of the system schematized in Fig. 5 can be assimilated as:

$$[T](s) = \begin{bmatrix} 1 & Z_s \\ 0 & 1 \end{bmatrix} \cdot \begin{bmatrix} 1 + \frac{1}{2}\left[RG + s\left(LG + RC\right) + s^2 LC\right] & R + sL \\ G + sC & 1 + \frac{1}{2}\left[RG + s\left(LG + RC\right) + s^2 LC\right] \end{bmatrix} \cdot \begin{bmatrix} 1 & 0 \\ \frac{1}{Z_L} & 1 \end{bmatrix}, \tag{19}$$

where $\begin{bmatrix} 1 & Z_s \\ 0 & 1 \end{bmatrix}$ and $\begin{bmatrix} 1 & 0 \\ \frac{1}{Z_L} & 1 \end{bmatrix}$ represents respectively the transfer matrices of the series impedance Z_s and the output shunt impedance Z_L. From the transfer matrix $[T](s)$ expressed in (19), one can demonstrate easily that the overall transfer function $H(s)$ can be formulated as follows:

$$H(s) = \frac{1}{[T]_{11}(s)} = \frac{1}{a_0(s) + a_1(s) \cdot s + a_2(s) \cdot s^2}, \tag{20}$$

where

$$a_0(s) = \frac{(2 + R \cdot G + 2 \cdot G \cdot Z_s)}{2} \cdot Z_L + \frac{(2 + R \cdot G)}{2} \cdot Z_s + R, \quad (21)$$

$$a_1(s) = \frac{(R \cdot C + L \cdot G + 2 \cdot C \cdot Z_s) \cdot Z_L}{2} + L + \frac{(R \cdot C + L \cdot G)}{2} \cdot Z_s, \quad (22)$$

$$a_2(s) = \frac{L \cdot C}{2} \cdot (Z_L + Z_s). \quad (23)$$

To confirm the efficiency of this transfer function model, let us see its time domain responses computed with Matlab and then compare with the results from the SPICE-ADS simulations. Thus, we will evaluate the examples of interconnection transient parameters as rise-/fall-times and the 50% propagation delay.

4. VALIDATION RESULTS

To give evidence to the relevance of the previous theoretic concepts, let us consider the arbitrarily folded microstrip interconnection line pictured in Fig. 6. This microstrip device was simulated in SPICE schematic environment of standard microwave electronic tool ADS from Agilent^{TM}.

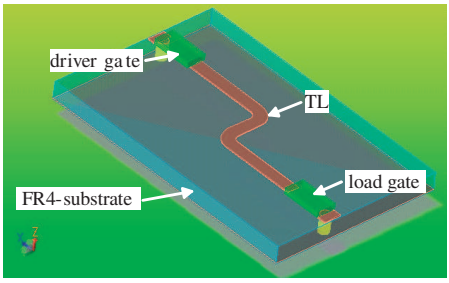

Figure 6. 3D-design of the simulated microstrip interconnection line.

This structure was printed on the FR4-substrate having physical characteristics and arbitrary chosen geometrical parameters summarized in Table 1.

Table 1. Physical characteristics of the tested microstrip line.

w	h	t	ε_r	$(\tan\delta)$
500 µm	625 µm	35 µm	4.4	0.012

By applying the RLCG-model extraction formulations introduced earlier in Section 2, one obtains the following per unit length values: $R_u = 16.6\,\Omega/\text{m}$, $L_u = 464.7\,\text{nH/m}$, $C_u = 74.7\,\text{pF/m}$ and $G_u = 5.6\,\text{mS/m}$. With this numerical value, we have implemented the above transfer function into Matlab program. Then, to generate the transient responses of the structure, a periodical trapezoidal pulse presenting the temporal characteristics (t_r: rise time, t_f: fall time, T_p: period, t_w: pulse time duration) with steady states $V_{low} = 0\,\text{V}$ and V_{high} normalized at 1 V addressed in Table 2 was considered as the input.

Table 2. Parameters of the considered input excitation signal.

t_r	t_f	T_p	t_w	V_{low}	V_{high}
100 ps	100 ps	1 ns	400 ps	0 V	1 V

Since the rise-/fall-time of the considered input signal is about 100 ps, according to (10), the maximum frequency required for the proposed polynomial model response have been estimated of about 3.5 GHz. We verify that it enables to generate transient response taking into account the propagating TEM-modes through the under test structure which is compliant with the second order transfer function expressed in (20). In order to demonstrate the adaptability of the proposed modelling method for various types of the load impedance, let us analyse the computed results first, for the resistive load ($Z_L = R_L$) and then, for the capacitive load ($Z_L = 1/(C_L \cdot p)$) in the next paragraphs. As aforementioned, the comparative results are referred with SPICE simulations run in ADS transient simulations regarding the physical parameters summed up in above Table 1.

4.1. Transient Responses for $Z_L = R_L$

It is interesting to note that the static gain of the overall understudy system (see Fig. 4) is equal to $H(0) = R_L/R_S$ when the source and load impedances are purely resistive. In the present case, we have changed the value of the resistive load $R_L = \{10\,\Omega, 500\,\Omega\}$ and the length of the microstrip line $d = \{8.5\,\text{mm}, 13.5\,\text{mm}\}$. So, one gets the comparative results plotted in Fig. 7. The proposed model responses are plotted in full lines and the ADS simulation results are in dashed lines.

One can see that the transient response generated from the proposed model agrees very well with the SPICE simulations. One observes that through the microstrip interconnection the pulse signal is significantly degraded. Here, with the two computation processes,

one evaluates rise-/fall-times of about $t_r \approx 0.14\,\text{ns}$ for $R_L = 500\,\Omega$ and $t_r \approx 0.43\,\text{ns}$ for $R_L = 10\,\Omega$. Then, one evaluates rise-/fall-time relative errors of about 1%.

4.2. Transient Responses for $Z_L = 1/(C_L \cdot p)$

In this case, Z_L is assumed as a capacitive load C_L. In order to show the interaction between these load values and the interconnect line, we have changed the values of the capacitive load $C_L = \{1\,\text{pF}, 10\,\text{pF}, 30\,\text{pF}\}$ and the lengths of the microstrip line $d = \{8.5\,\text{mm}, 13.5\,\text{mm}\}$ to demonstrate the flexibility of the proposed modelling process. As consequence, one gets the comparative results displayed in Fig. 8 below. The proposed model responses are plotted in full lines and the ADS simulation results are in dashed lines.

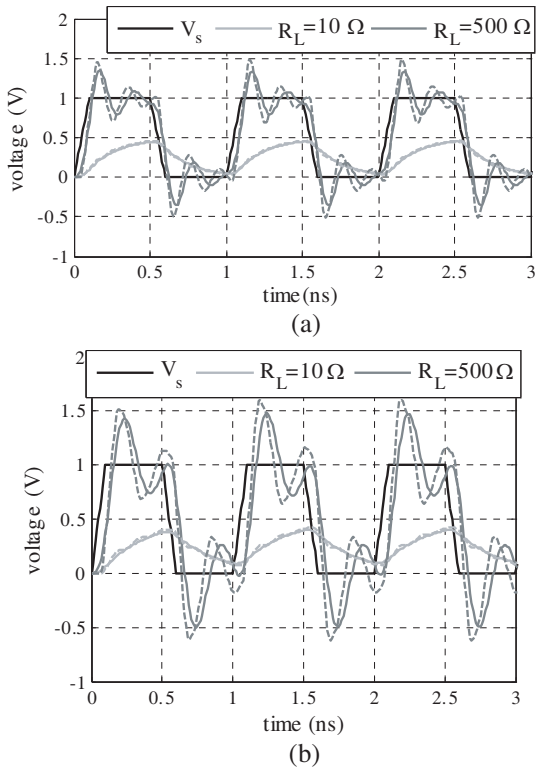

Figure 7. Transient responses of the microstrip structure shown in Fig. 6 for different values of the load gate resistance R_L for (a) $d = 8.5\,\text{mm}$ and (b) $d = 13.5\,\text{mm}$.

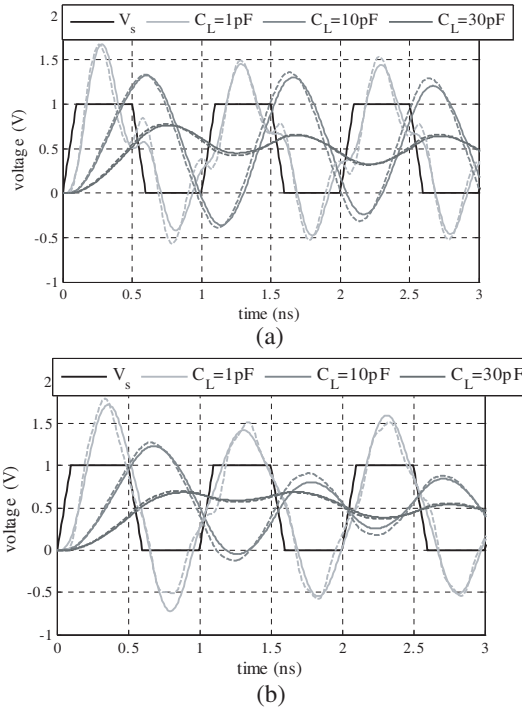

Figure 8. Transient responses of the microstrip structure shown in Fig. 6 for different values of the capacitive load C_L: (a) $d = 8.5\,\text{mm}$ and (b) $d = 13.5\,\text{mm}$.

One can see that the output is completely distorted for the capacitive load C_L higher than 1 pF. One evaluates here a 50% propagation delay of about $T_{p50\%} = \{80\,\text{ps}, 240\,\text{ps}, 440\,\text{ps}\}$ respectively for $C_L = \{1\,\text{pF}, 10\,\text{pF}, 30\,\text{pF}\}$.

For the both examples of the performed validation results, one points out that the computation time with the proposed method is in order of tens microseconds. The presented method is practically simpler than most of 3-D EM solver ones as the example of the TD integral equation presented in [34].

5. CONCLUSION

A transfer function modelling method of the millimetre interconnection for the high-speed integrity analysis in the RF-/digital PCB is investigated. The established model is based on the exploitation of the electrical RLCG-model transfer matrix which was assumed as its

second order polynomial linear model.

To evidence the functionality of the introduced method, a microstrip interconnection TL driven and loaded by the logic gates was considered and analysed. It was described that the per unit length equivalent model parameters were determined from the TL physical and the geometrical parameters as the substrate permittivity and height, and the line width and length. Then, the equivalent transfer function linear model of the overall system composed of a TL combined with the logic gates is mathematically established. Thus, for the testing process, it was excited with a periodical trapezoidal pulse voltage with 2 Gbits/s rate. So, good agreement between the transient responses from the established transfer function calculated with Matlab and those from SPICE simulations of the overall structure was found. It was shown that the microstrip interconnection responses are completely degraded. Then, after the sweep of the load impedance values assigned as resistance and capacitance loads, one observes also that the calculated transient results remain well-correlated to the simulations.

One emphasizes that the design and the simulation of this type of microwave digital interconnections become very difficult to carry out when the circuit is composed of thousands of logic gates. For this reason, it seems important to exploit the proposed modelling method for the prediction the analogue-digital signal behaviours along the interconnections. Thanks to the accuracy and the computation time gain, we think that the proposed method can be a good candidate for the modelling of the complex structure of the interconnection circuitry in the high density integrated circuit as the clock distribution networks.

In the continuation of this work, one plans to improve this method for the estimation of the RF-microwave and digital electronic device interconnection effects by taking into account the non-uniformity of the TL as introduced in [35] and the eventual crosstalk with the neighbourhood TLs [36]. Then, we would employ the proposed method to the development of the equalization technique with the NGD circuit for the reduction of the correction of the digital signal degradation with MMIC and digital integrated systems.

REFERENCES

1. International Technology Roadmap for Seminconductors Update Overview, http://www.itrs.net/Links/2009ITRS/Home2009.htm.
2. Deutsch, A., "High-speed signal propagation on lossy transmission lines," *IBM J. Res. Develop.*, Vol. 34, No. 4, 601–615, Jul. 1990.
3. Celik, M., L. Pileggi, and A. Odabasioglu, *IC Interconnect*

Analysis, 1-4020–7075-6, Kluwer Academic Publisher, Dordrecht, 2002.

4. Ligocka-Wardzinska, A. and W. Bandurski, "Sensitivity of output response to geometrical dimensions in VLSI interconnects," *Proc. of 13th IEEE Workshop SPI*, 1–4, Strasbourg, France, May 2009.
5. Chiu, C.-N. and I.-T. Chiang, "A fast approach for simulating long-time response of high-speed dispersive and lossy interconnects terminated with nonlinear loads," *Progress In Electromagnetics Research*, Vol. 91, 153–171, 2009.
6. Ghoneima, M., Y. Ismail, M. M. Khellah, J. Tschanz, and V. De, "Serial-link bus: A low-power on-chip bus architecture," *IEEE Trans. CAS I*, Vol. 56, No. 9, 2020–2032, Sep. 2009.
7. Hwang, M.-E., S.-O. Jung, and K. Roy, "Slope interconnect effort: Gate-interconnect interdependent delay modeling for early CMOS circuit simulation," *IEEE Trans. CAS I*, Vol. 56, No. 7, 1428–1441, Jul. 2009.
8. Elmore, W. C., "The transient response of damped linear networks," *J. Appl. Phys.*, Vol. 19, 55–63, Jan. 1948.
9. Wyatt, J. L., *Circuit Analysis, Simulation and Design*, Elsiever Science, North-Holland, The Netherlands, 1978.
10. Kahng, A. B. and S. Muddu, "An analytical delay model of RLC interconnects," *IEEE Trans. Computed-Aided Design*, Vol. 16, 1507–1514, Dec. 1997.
11. Ismail, Y. I. and E. G. Friedman, "Effects of inductance on the propagation, delay and repeater insertion in VLSI circuits," *IEEE Trans. VLSI Sys.*, Vol. 8, No. 2, 195–206, Apr. 2000.
12. Ismail, Y. I., E. G. Friedman, and J. L. Neves, "Equivalent Elmore delay for RLC trees," *IEEE Trans. CAD*, Vol. 19, No. 1, 83–97, Jan. 2000.
13. Ligocka, A. and W. Bandurski, "Effect of inductance on interconnect propagation delay in VLSI circuits," *Proc. of 8th IEEE Workshop SPI*, 121–124, May 9–12, 2004.
14. Basl, P. A. W., M. H. Bakr, and N. K. Nikolova, "Efficient transmission line modeling sensitivity analysis exploiting rubber cells," *Progress In Electromagnetics Research B*, Vol. 11, 223–243, 2009.
15. Xie, H., J. Wang, R. Fan, and Y. Liu, "Study of loss effect of transmission lines and validity of a Spice model in electromagnetic topology," *Progress In Electromagnetics Research*, Vol. 90, 89–103, 2009.
16. Hammerstad, E. and O. Jensen, "Accurate models for microstrip

computer aided design," *IEEE Trans. MTT*, 407–409, 1980.

17. Hammerstad, E. O., "Equations for microstrip circuit design," *Proc. of 5th EuMC*, 268–272, Sep. 1975.
18. Marks, R. B. and D. F. Williams, "Interconnection transmission line parameter characterization," *Proc. of 40th ARTG Conf. Dig.*, 88–95, Orlando, FL, USA, Dec. 1992.
19. Marks, R. B. and D. F. Williams, "Characteristic impedance determination using propagation constant measurement," *IEEE Mic. Guided Wave Lett.*, No. 6, 141–143, Jun. 1991.
20. Eisenstadt, W. R. and Y. Eo, "*S*-parameter-based IC interconnect transmission line characterization," *IEEE Trans. Comp. Hybrids Manuf. Technol.*, Vol. 15, 483–490, Aug. 1992.
21. Deutsch, A., R. S. Krabbenhoft, K. L. Melde, C. W. Surovic, G. A. Katopis, G. V. Kopcsay, Z. Zhou, Z. Chen, Y. H. Kwark, T.-M. Winkel, X. Gu, and T. E. Standaert, "Application of the short-pulse propagation technique for broadband characterization of PCB and other interconnect technologies," *IEEE Trans. EMC*, Vol. 52, 266–287, Feb. 2010.
22. Cong, J., L. He, C.-K. Koh, and P. Madden, "Performance optimization of VLSI interconnect," *Integration VLSI J.*, Vol. 21, 1–94, Nov. 1996.
23. Yun, B. and S. S. Wong, "Optimization of driver preemphasis for on-chip interconnects," *IEEE Trans. CAS I*, Vol. 56, No. 9, 2033–2041, Sep. 2009.
24. Rosenfeld, J. and E. G. Friedman, "Design methodology for global resonant H-tree clock distribution networks," *IEEE Trans. VLSI Systems*, Vol. 15, No. 2, 135–148, Feb. 2007.
25. Awwad, F. R., M. Nekili, V. Ramachandran, and M. Sawan, "On modeling of parallel repeater-insertion methodologies for SoC interconnects," *IEEE Trans. CAS I*, Vol. 55, No. 1, 322–335, Feb. 2008.
26. Ravelo, B., A. Perennec, and M. Le Roy, "Experimental validation of the RC-interconnect effect equalization with negative group delay active circuit in planar hybrid technology," *Proc. of 13th IEEE Workshop SPI*, Strasbourg, France, May 2009.
27. Ravelo, B., A. Perennec, and M. Le Roy, "New technique of inter-chip interconnect effects equalization with negative group delay active circuits," *VLSI*, Z. F. Wang (ed.), Chap. 20, 409–434, INTECH, Feb. 2010.
28. Zhang, J. and T. Y. Hsiang, "Extraction of subterahertz transmission-line parameters of coplanar waveguides," *PIERS*

Online, Vol. 3, No. 7, 1102–1106, 2007.

29. Kashyap, C. V., C. J. Alpert, F. Liu, and A. Devgan, "Closed-form expressions for extending step delay and slew metrics to ramp inputs for RC trees," *IEEE Trans. CADICAS I*, Vol. 23, No. 4, 509–516, Apr. 2004.
30. Kirschning, M. and R. H. Jansen, "Accurate model for effective dielectric constant with validity up to millimeter-wave frequencies," *Electronics Letters*, Vol. 18, 272–273, 1982.
31. Pozar, D. M., *Microwave Engineering*, 2nd edition, 9–21 & 154–166, John Wiley, 1998.
32. Pucel, R. A., D. J. Massé, and C. Hartwing, "Losses in microstip," *IEEE Trans. MTT*, Vol. 16, No. 6, 342–350, 1968.
33. Chen, C., J. Lillis, S. Lin, and N. Chang, *Interconnect Analysis and Synthesis*, Wiley, New York, 2000.
34. Zhang, G. H., M. Y. Xia, and X. M. Jiang, "Transient analysis of wire structures using time domain integral equation method with exact matrix elements," *Progress In Electromagnetics Research*, Vol. 92, 281–298, 2009.
35. Torrungrueng, D. and S. Lamultree, "Equivalent graphical solutions of terminated conjugately characteristic-impedance transmission lines with non-negative and corresponding negative characteristic resistances," *Progress In Electromagnetics Research*, Vol. 92, 137–151, 2009.
36. Roy, A., S. Ghosh, and A. Chakrabarty, "Simple crosstalk model of three wires to predict near-end and far-end crosstalk in EMI/EMC environment to facilitate EMI/EMC modeling," *Progress In Electromagnetics Research B*, Vol. 8, 43–58, 2008.